STM characterization of Cu thin films grown by direct ion deposition

Joshua M. Pomeroy, Aaron Couture, Joachim Jacobsen[1], Colin C. Hill, James P. Sethna, Barbara H. Cooper[2], and Joel D. Brock
Cornell Center for Materials Research,
Clark Hall, Cornell University,
Ithaca, NY 14853 USA
[1]currently with Haldor Topsøe A/S, Denmark
[2]deceased August 9, 1999

ABSTRACT

In certain cases, the incidence energy of constituent atoms activates an atomistic insertion mechanism, which decreases the surface roughness of metal thin films. In an effort to probe this effect, homoepitaxial copper films were grown using a mass/energy selected direct ion deposition technique that allows precise control of the incidence energy. Surface roughness is measured using a Scanning Tunneling Microscope (STM) within the same UHV surface analysis system. The activation of the insertion mechanism near 20 eV triggers smoother crystal growth. The beneficial effects begin to be obscured by adatom/vacancy creation near 30 eV. A sophisticated Kinetic Monte Carlo/Molecular Dynamics (KMC-MD) model supports this interpretation.

INTRODUCTION

Efforts to produce smooth thin films fall into two general categories, those that produce a thermal vapor, which condenses on the sample substrate; and those which produce atoms, ions, or clusters with a hyperthermal energy [1]. Considerable attention and effort has led to a detailed understanding of thermal growth [2], but such understanding has not been achieved for hyperthermal deposition.

Hyperthermal deposition is fundamentally different from thermal deposition due to the increased incidence velocity of the constituent atoms. Thermal deposition is often modeled as a gentle landing or, in some cases, sticking to the first point of contact (Ballistic Deposition) [3]. During hyperthermal deposition, the significantly increased incidence velocities provide enough energy to rearrange the atoms at the impact site into configurations unattainable by thermal kinetics.

Two mechanisms that are important at hyperthermal energies are atomic insertions and the formation of adatom/vacancy pairs. Insertions can occur when an atom is incident within a few atomic positions above an atomic step and has enough energy to implant itself into the surface without creating any defects, usually by shifting atoms outward at the step edge. This mechanism, which is independent of sample temperature, tends to smooth the surface. Adatom/vacancy pairs form when the incident atom has enough energy to dislodge surface atoms from their sites, which increases the surface roughness, but also increases the nucleation density.

Experimental efforts to decipher the role of incidence energy during the evolution of thin film growth include supersonic jets, Ion Beam Assisted Deposition (IBAD), and direct ion deposition [1,4]. While some success has been enjoyed in controlling morphological transitions [5], fundamental understanding has been limited to sub-monolayer deposition despite continued endeavors [6].

Efforts presented here explore the role of incidence energy in determining growth modes and surface morphology by using a precision hyperthermal energy metal ion beam-line and a STM. Specifically, the dependence of surface roughness on incident energy is explored, and explained with the assistance of various computer simulations and previously published work by other authors.

EXPERIMENTAL DETAILS

Experiments were performed in an UHV system consisting of three isolated sections. The hyperthermal energy metal ion beam is split two thirds of the way down the beam-line by a gate valve to form the first section. The last third of the ion beam leads into the deposition chamber, and focuses onto a five-axis variable temperature manipulator. This section is equipped with Auger Electron Spectroscopy (AES), and other necessary equipment for sample and STM tip preparation and analysis. The final section is isolated from the previous by another gate valve, and connected via a narrow bellows that allows for sample transfer. The final section houses the UHV Omicron STM-1, and sits on a vibration reduction table.

Sample preparation of the Cu(111) crystal included repeated cycles of 500 eV Ar^+ ion erosion and annealing to 750° C. Flatness and cleanliness were verified by AES and by STM prior to depositing with the ion source. Once the sample was clean, it was isolated in the STM chamber at $7x10^{-11}$ Torr while the ion beam was being started and tuned, typically an hour.

The custom-built ion beam line was specifically designed for producing ion beams with an extremely narrow distribution of kinetic energies. Ions are formed in a Penning cell, then extracted through electrostatic lenses, static deflection plates, and a mass selecting magnet. The magnet refocuses the ion beam about a central energy satisfying the Lorentz condition while aperturing the beam to single AMU resolution in mass, and (delta E)/E ~ 1/10 in energy resolution. Ion beam purity was characterized by AES. The energy resolution was characterized by measuring total current versus reverse bias voltage. The spatial distribution of the beam was measured by scanning an aperture and de-convoluting [7].

Once the ion beam has stabilized and the sample has been prepared, the sample is transferred via a network of wobble-sticks and transfer arms to the manipulator. Deposition is performed at normal incidence by maintaining a 100 nA dc ion current on the sample at room temperature. Based on the cross-sectional analysis of the ion beam, a thirty-minute deposition corresponds to approximately four monolayers. AES following deposition does not reveal any measurable impurities or background gas contamination.

Finally, the sample is returned to the STM, where scanning begins following a period of thermal equilibration, which is approximately 10 minutes. Sample topographs are taken sequentially with uni-axial translations of a few hundred nanometers between each image over a period of six to eight hours.

DATA

STM topographs of (111) copper films grown by direct ion beam deposition at several different energies are presented in Figure 1. The step edges seen are single atomic height steps, and darker colors represent lower levels. All four images are 200x200 nm in size.

| (a) | (b) | (c) | (d) |
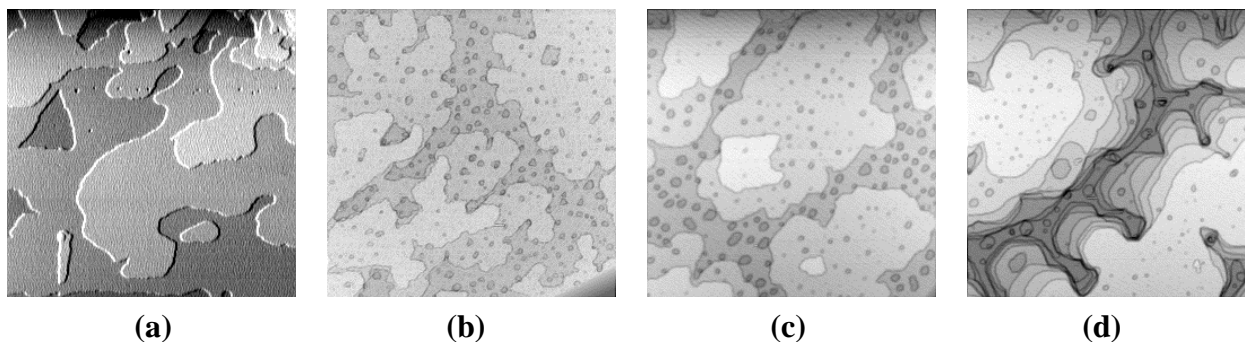
Figure 1. Copper thin films deposited on Cu(111) by direct ion deposition at 20 eV (a), 40 eV (b), 60 eV (c), and 100 eV (d) at room temperature. All four STM topographs are 200x200 nm and are taken after ~4 monolayers of deposition.

At 20 eV (Figure 1a) the film is smoother than at higher energies. The few vacancy islands visible tend to be quite small. In studies of Pt(111) surfaces, step edges aligned with low index directions [8]. Here the step edges wander smoothly and form complex contours.

In contrast to the 20 eV samples, films grown at 40 eV (Figure 1b) exhibit a high density of vacancy islands. These vacancy islands are nearly uniform in size, particularly islands on the same atomic level. In some cases vacancy islands in the lowest levels have pinned steps on higher levels, leading to increased complexity of the contours.

At 60 eV (Figure 1c), the vacancy islands are still coarser than at lower energies. In particular, vacancy islands in the lowest atomic levels are noticeably larger than vacancy islands in the topmost layer. In general, the contours in the 60 eV images are similar in complexity to the 40 eV images.

The surface morphology of films grown at 100 eV (Figure 1d) is noticeably different. While only four monolayers of material have been deposited, at least nine different layers are exposed. In some cases, all nine of these layers bunch up tightly around a single pinhole with a narrow neck drawing out to more relaxed contours. The large features on the surface look more like plateaus than the "wedding cake" morphology or 2D layers observed at lower energies. Deep trenches completely separate these objects.

DISCUSSION

In an initial effort to quantify the changes in surface morphology with increasing incident ion energy, measured RMS surface roughness values are plotted as a function of energy (Figure 2). The values are averaged over many different areas on the film. Roughness has been calculated for two different sized areas to check for strong dependence on sample size. Triangles represent the mean value for RMS roughness calculated on 100x100 nm sized areas, and circles for 200x100nm areas. The error bars represent the standard deviation. Between 20 and 60 eV, the RMS roughness increases with a gentle slope, but between 60 eV and 100 eV the RMS roughness increases significantly.

To identify specific atomistic mechanisms that trigger the macroscopic morphological changes, Molecular Dynamics (MD) simulations of the atomic collision processes were performed (details are presented in [9]). While the insertion mechanism does not show a strong dependence in this energy range, adatom/vacancy pair production rapidly increases near 20 eV.
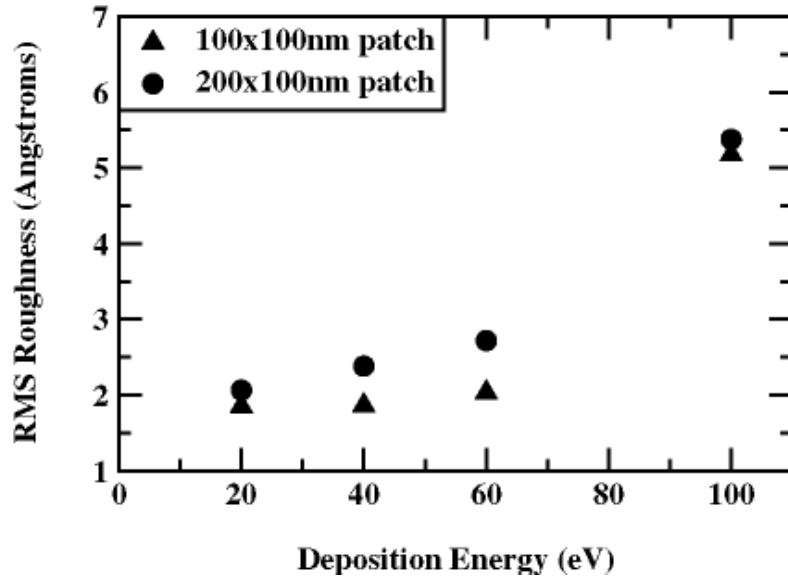
Figure 2. RMS roughness of both 100x100nm and 200x100nm patches calculated from many STM topographs taken at each of the deposition energies. The roughness increases gently from 20 to 60 eV in energy, but then turns increases markedly between 60 and 100 eV.

consistent with the gentle increase in the RMS roughness between 20 and 60 eV in the STM data. Adatom/vacancy production definitely contributes to vacancy island formation between 20 and 40 eV, but atomic sputtering may also be important.

Re-sputtering is addressed in molecular dynamics studies by Zhou and Wadley ([10] Figure 8). They simulate atomic collisions of copper ions on Cu(111) from 0 to 50 eV at various incidence angles and analyze the probability for reflection or re-sputtering. The sputter yield is found to be ~0.05 for 50 eV copper atoms at normal incidence, which decreases to less than 0.01 at 30 eV ([10] Figure 9). Therefore, at 30 eV, approximately 30 adatom/vacancy pairs are generated for each re-sputtered atom. The presence of vacancy islands at 40 eV is due solely to adatom/vacancy formation.

Attributing a large number of vacancy islands to adatom/vacancy production in the absence of a large number of adatom islands is not contradictory. The Cu(111) surface is known to have a large difference in the energetic barriers for adatom diffusion and vacancy diffusion, as well as edge and interlayer diffusion rates [11]. Adatom diffusion is so fast that atoms will hop 10^{10} times at room temperature before a vacancy diffuses once, and an adatom at a straight step edge will descend only 1 in 10^6 times. Consequently, an adatom remains trapped in the layer it is introduced, wandering until it encounters an uphill step or another adatom. The probability of finding a step is much higher than encountering another walker in this flux regime, so small adatom islands are rare. On the other hand, vacancies move slowly developing a high vacancy density, so that the probability of any given vacancy encountering a second vacancy is higher than encountering a downhill step. As a result, the surface is decorated with vacancy islands, but very few adatom islands.

While adatom/vacancy atomistics describe the changes in morphology from 20 eV to 60 eV, the rapid increase in roughness between 60 and 100 eV requires an additional mechanism. While Zhou and Wadley did not address re-sputtering effects above 50 eV, it is clear that sputter yields increase quickly above 50 eV. In work done on Pt(111) (whose atomistics are similar to Cu(111) [12]) sputter and adatom/vacancy yields of 1 were observed at 200 eV for Xe+ [13]. This suggests that the dramatic morphological change between 60 eV and 100 eV in Figure 1 is due to the onset of sputter erosion.
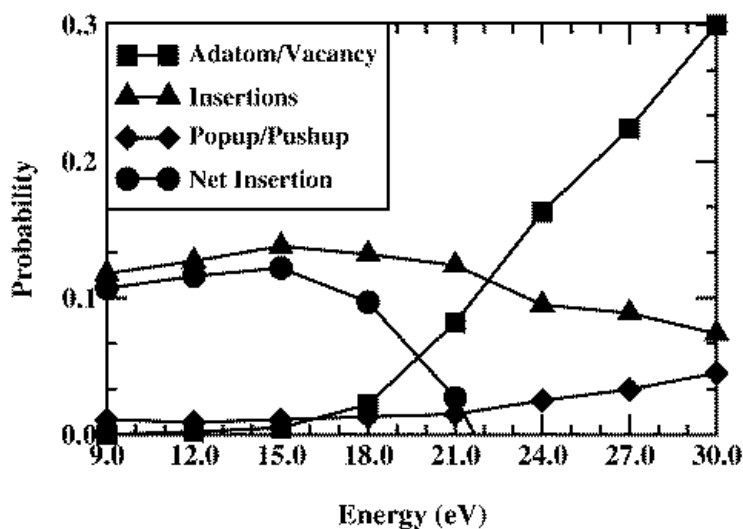
Figure 3. Results from a molecular dynamics simulation of a copper atoms impinging on a Cu(111) surface. These results suggest a threshold for adatom/vacancy pair production near 20 eV. The simulation also suggests an insertion dominated energy range below 20 eV, which could lead to smooth microscopic growth.

In an effort to include the effect of both collisional dynamics and surface kinetics, the MD previously mentioned was embedded in a Kinetic Monte Carlo simulation (KMC-MD details in [9]). While efforts to model exact experimental conditions are ongoing, initial results at 80 K, 1 monolayer/s deposition flux, and up to 40 eV have produced promising results. The simulated RMS roughness of films grown by KMC-MD is shown in Figure 4. These results suggest an optimum energy near 25 eV for thin film growth, where the surface roughness is minimized by insertions before the onset of adatom/vacancy production.

CONCLUSIONS

Copper thin films grown by direct ion deposition show a strong morphological dependence on incident ion energy. Films grown at 20 eV are smooth due to high adatom diffusion rates and atomistic insertion mechanisms. Films grown at 40 eV exhibit a high density of vacancy islands of nearly uniform size, whose presence is attributed to the onset of adatom/vacancy production near 20 eV based on molecular dynamics simulations. With increasing energy, the vacancy islands are observed to grow coarser at the lower levels, contributing to an increasing RMS roughness that is consistent with production rates predicted by molecular dynamics simulations.

The transition from a predominantly two-dimensional morphology decorated with vacancy islands at 60 eV to a plateau-like three-dimensional morphology at 100 eV is attributed to the onset of sputter roughening during growth. The exact nature by which the morphology develops requires additional investigation.

As part of an effort to correlate atomistic mechanisms with morphological transitions, a KMC-MD simulation has been developed. Results from this simulation suggest a possible optimal energy window for thin film growth near 25 eV in a diffusion-limited regime. Experimental efforts to observe this effect are planned.

ACKNOWLEDGEMENTS
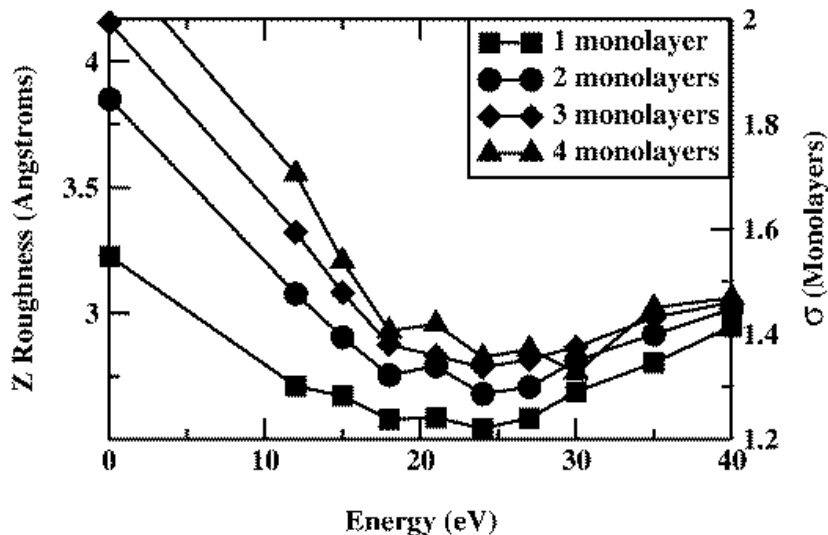
Figure 4. RMS roughness plotted as a function of energy for the first four monolayers of deposition in a Kinetic Monte Carlo and Molecular Dynamics hybrid simulation (KMC-MD). Growth is simulated at 80 K at 1 monolayer/s on a 80x80 Cu(111) surface. Results suggest an optimal energy window for thin film growth near 25 eV.

REFERENCES

1. T. Michely, M. Kalff, and G. Comsa in *Mechanisms and Principles of Epitaxial Growth in Metallic Systems*, edited by T. Wille; C. Burmester; K. Terakura; G. Comsa; and E. Williams, (Mater. Res. Soc. Proc. **278**, Warrendale, PA, 1998) pp. 179-193.
2. G. Rosenfeld, B. Poelsema, and G. Comsa, in *The Chemical Physics of Solid Surfaces Vol.8: Growth and Properties of Epitaxial Layers*, edited by D. King and D. Woodruff, (Elsevier, Amsterdam 1997) pp. 66-101
3. F. Family and T. Vicsek, J. Phys. A **18,** L75-L81 (1985).
4. J. Greene, S.A. Barnett, J.-E. Sundgren, and A. Rockett, in *Ion Beam Assisted Film Growth,* edited by T. Itoh (Elsevier, Amsterdam 1989) p. 101.
5. G. Rosenfeld, N. Lipkin, W. Wulfhekel, J. Kliewer, K. Morgenstern, B. Peolsema, and G. Comsa, Appl. Phys. A **61,** 455 (1995); W. Wulfhekel, N. Lipkin, J. Kliewer, G. Rosenfeld, L. Jorritsma, B. Poelsema, and G. Comsa, Surf. Sci. **348,** 277 (1996); B. Karr, Y. Kim, I. Petrov, D. Bergstrom, D. Cahill, J. Greene, L. Madsen, and J. Sundgren, J. Appl. Phys. **80,** 12 (1996); T. Minvielle, R. White, and R. Wilson, J. Appl. Phys. **79** (8), 2750 (1996).
6. I. Petrov, F. Adibi, and J. Greene, Appl. Phys. Lett. **63** (1), 36 (1993).
7. C. Sosolik, A. Lavery, E. Dahl, and B. Cooper, Rev. Scient. Instr. **71,** 9 3326 (2000).
8. T. Michely, T. Land, U. Littmark, and G. Comsa, Surf. Sci. **272,** 204 (1992).
9. J. Jacobsen, B. Cooper, and J. Sethna, Phys. Rev. B **58** (23), 15847 (1998).
10. X. Zhou and H. Wadley, Surf. Sci. **430,** 58-73 (1999).
11. P. Stolze, J. Phys. Condens. Matter **6,** 9495 (1994).
12. J. Naumann, J. Osing, A. Quinn, I. Shvets, Surf. Science **388,** 212 (1997).
13. T. Michely and C. Teichert, Phys. Rev. B **50** (15), 11156 (1994).